Springer

Journal of
Mechanical
Science and
Technology

Journal of Mechanical Science and Technology 23 (2009) 3349~3356

www.springerlink.com/content/1738-494x
DOI 10.1007/s12206-009-0913-3

Bubble growth in mold cavities during microcellular injection molding processes †

Yongrak Moon[1], Kyoung-soo Lee[2] and Sung W. Cha[2,*]

[1]*Department of Mechanical & Industrial Engineering, University of Toronto, 5 King's College, M5S 3G8, Canada*
[2]*Department of Mechanical Engineering, Yonsei University, Seoul, 120-749, Korea*

(Manuscript Received June 7, 2007; Revised August 20, 2009; Accepted August 27, 2009)

Abstract

Bubble nucleation and growth are the key steps in polymer foam generation processes. The mechanical properties of foam polymers are closely related to the size of the bubbles created inside the material, and most existing analysis methods use a constant viscosity and surface tension to predict the size of the bubbles. Under actual situations, however, when the polymer contains gases, changes occur in the viscosity and surface tension that cause discrepancies between the estimated and observed bubble sizes. Therefore, we developed a theoretical framework to improve our bubble growth rate and size predictions, and experimentally verified our theoretical results using an injection molding machine modified to make microcellular foam products.

Keywords: Bubble Growth; Bubble growth rate; Injection molding; Microcellular foam products; Polymer foam

1. Introduction

Polymers are limited resources, and considerable effort has been directed toward developing methods to reduce their consumption. One such method reduces the quantity of raw materials required to manufacture polymers by using polymer foam. Initially, chemical blow agents were used to create the foam, but because of the harmful effects of chemical substances on the environment, a microcellular foaming process, which is environmentally friendly, has recently been developed [1]. Compared to chemical foaming, microcellular foaming has less effect on the environment since it uses CO_2 and N_2.

The most important consideration when producing microcellular foam products is the resulting mechanical properties. One of the goals of microcellular foam is to maintain the mechanical properties of standard polymers while reducing the required quantity of raw materials. One important factor that influences the mechanical properties is the morphology of the cells generated inside the products, such as the cell size, shape, and density [2, 3].

When using an ultrafine foaming method in an injector, it is necessary to manage the size and number of bubbles in the inner body of the product to meet the needs of the customer. Several studies on the mechanical properties of a product manufactured using an ultrafine foaming method have focused mainly on batch tests using high-pressure containers. Other studies of continuous processes, such as the press and injection method, have been performed under specific conditions, such as those of a capillary die, because many parameters in the manufacturing process are uncontrollable. Although many commercial analysis simulation tools have been developed to predict the size of the bubbles that grow in polymers inside the molds, the analysis results typically do not match the size of the bubbles observed in actual products. This is because the amount of theoretical research on the

† This paper was recommended for publication in revised form by Associate Editor Dae-Eun Kim
*Corresponding author. Tel.: +82 2 2123 4811, Fax.: +82 2 364 9364
E-mail address: swcha@yonsei.ac.kr

growth of bubbles that considers the flow of the polymer inside the mold is limited. We therefore propose a bubble model that includes any gas growth inside the mold using a theoretical approach that considers the flow properties of the polymer and an estimation technique developed to provide more accurate predictions by comparing the results of existing analysis tools with the actual size of bubbles observed on a metal specimen.

2. Theory

2.1 Microcellular foaming technology

Conventional foaming technologies use physical blowing agents with nucleating or chemical blowing agents that induce heterogeneous nucleation in the material at a fixed number of sites. The actual number of cell sites is directly related to the quantity of the nucleating agents added. Heterogeneous nucleation produces a foam material characterized by large non-uniform cells, and the lack of cell size uniformity is due to the relatively slow nucleation rate. Typically, conventional foams have cells ranging from 250 μm to 1 mm in diameter [4].

Microcellular foams have uniform cell diameters that are less than 100 μm. This cell structure can only be obtained through the simultaneous generation of a high number of nucleation sites. The requirement for very high nucleation rates and the resultant creation of a large number of nucleation sites necessitate a fundamental change in the way in which the cells are nucleated [5, 6]. Microcellular foam is produced when the cell nucleation rate is both extremely high (orders of magnitude greater than conventional foaming processes) and much greater than the diffusion rate of the blowing agent into the cells. Under these conditions, an extremely large number of cells will be created before any cell growth occurs. Consequently, when the blowing agent diffusion begins to dominate the foam creation process, all cell sites will begin to grow at the same time and at approximately the same rate, resulting in a material characterized by a large number of evenly distributed, uniformly sized, microscopic cells [7].

2.2 Bubble growth theory

The growth process of a critical nucleus is as follows:

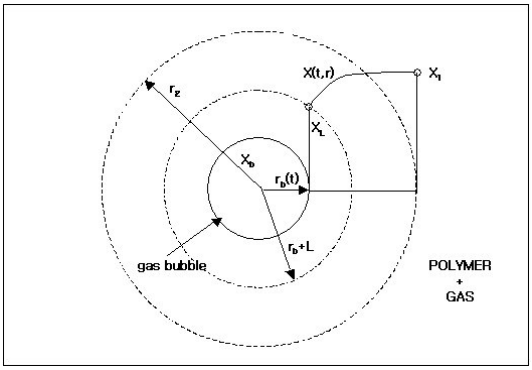

Fig. 1. Schematic representation of a model for spherical bubble growth in a supersaturated liquid.

(1) Gas is diffused from the polymer into bubbles
(2) The pressure inside the bubbles rises
(3) The bubbles expand by pushing the surrounding liquid polymer outward.

Fig. 1 shows a bubble that is growing. A depleted zone L surrounds the bubble, where the gas concentration is lower than the initial supersaturated concentration X_1 as a result of mass transfer. The spherical diffusion boundary r_2 is an area where diffusion across the boundary does not occur. To interpret the growth of bubbles, we require the following assumptions:

(1) The resin into which gas is dissolved is incompressible
(2) The size of the diffusion boundaries is determined by the number of bubble nuclei
(3) The number of bubbles in a unit mass of polymer resin remains constant during the growth
(4) Gas in the liquid is regarded as an ideal gas.

The equation that governs the transfer of mass can be expressed using Fick's second law for a spherical coordinate system [8, 9],

$$\frac{\partial X}{\partial t} = D\left(\frac{\partial^2 X}{\partial r^2} + \frac{2}{r}\frac{\partial X}{\partial r}\right) \tag{1}$$

where X is the gas concentration, t is time, and D is the constant of gas diffusivity in the melting polymer.

Let us assume that this relationship can be described by Henry's law,

$$X_L = \frac{P_b}{K} \tag{2}$$

where K is the Henry's law constant. The initial and boundary conditions are [10]

$$X(0,r_b^*)=\frac{P_b^*}{K} \tag{3}$$

$$X(0,r_2^*)=X_1 \tag{4}$$

$$X(t,r_b)=\frac{P_b}{K} \tag{5}$$

$$\frac{\partial X(t,r_2)}{\partial r}=0 \tag{6}$$

where r_b* is the critical nucleus radius, P_b* is the pressure in the critical nucleus, and r_2* is the critical nucleus diffusion boundary. Eqs. (5) and (6) are transfer boundary conditions, where X (t, r_b) is variable during the nucleus growth and r_2 is the bubble diffusion boundary at an arbitrary time t.

The mass conservation equation for the gas in the bubble is

$$\frac{d}{dt}(\frac{4\pi}{3}r_b^3X_b)=4\pi r_b^2D(\frac{\partial X}{\partial r})_{r=r_b} \tag{7}$$

where X_b, which is the gas concentration in the bubble, assumed to be ideal, may be rewritten as

$$X_b=\frac{n_b}{V_b}=\frac{P_b}{RT} \tag{8}$$

The continuity and motion equations for the liquid phase in spherical coordinates, assuming a constant density and spherical symmetry, are

$$\rho(\frac{\partial v}{\partial t}+v\frac{\partial v}{\partial r})= -\frac{\partial P}{\partial r}+\eta(\frac{\partial^2 v}{\partial r^2}+\frac{2}{r}\frac{\partial v}{\partial r}-\frac{2v}{r^2}) \tag{9}$$

$$\frac{1}{r^2}\frac{\partial}{\partial r}(r^2v)=0 \tag{10}$$

$$v=\dot{r} \tag{11}$$

where η is the viscosity and ρ is the density. Eq. (10) can be rewritten as

$$\frac{\partial v}{\partial r}=-\frac{2v}{r} \tag{12}$$

$$\frac{\partial^2 v}{\partial r^2}=\frac{2v}{r^2}-\frac{2}{r}(\frac{\partial v}{\partial r}) \tag{13}$$

Substituting Eqs. (12) and (13) into Eq. (9) gives

$$\frac{\partial v}{\partial t}+v\frac{\partial v}{\partial r}=-\frac{1}{\rho}\frac{\partial P}{\partial r} \tag{14}$$

The following equations can also be derived using the overall integral continuity equation, Eq. (12):

$$vr^2=\dot{r}_b r_b^2 \qquad r\ge r_b(t) \tag{15}$$

$$\frac{\partial v}{\partial t}=\frac{r_b^2}{r^2}\ddot{r}_b+(\frac{2r_b}{r^2}-\frac{2r_b^2}{r^3})\dot{r}_b^2 \tag{16}$$

$$\frac{\partial v}{\partial r}=-2\frac{r_b^2}{r^3}\dot{r}_b \tag{17}$$

$$-\frac{1}{\rho}\int_{P_1}^{P_0}dP=\int_{r_b}^{\infty}(\frac{\partial v}{\partial t}+v\frac{\partial v}{\partial r})dr \tag{18}$$

where P_0 is the external pressure of the bubble and P_1 is the surface pressure in the bubble. Substituting Eqs. (15), (16), and (17) into Eq. (18) gives

$$\frac{P_1-P_0}{\rho}=r_b\ddot{r}_b+\frac{1}{2}\dot{r}_b^2 \tag{19}$$

$$P_b=P_1+\frac{2r}{r_b}-2\eta(\frac{\partial v}{\partial r})_{r=r_b} \tag{20}$$

Substituting Eqs. (17) and (20) into Eq. (19) gives

$$P_b=P_0+\frac{2r}{r_b}+\rho(r_b\ddot{r}_b+\frac{1}{2}\dot{r}_b^2)+4\eta\frac{\dot{r}_b}{r_b} \tag{21}$$

In an actual foaming process, myriad bubbles grow simultaneously in a limited space so that their growth differs from that of bubbles in infinite space. Ignoring coalescence resulting from the merging of a certain number of bubbles in the limited space, the number of bubbles per unit mass is constant and each bubble grows independently [11].

3. Bubble growth in microcellular injection molding processes

3.1 Viscosity change in a polymer/Gas mixture

When processing microcellular foam polymer products, one of the most important factors is the specific characteristic of the rheology, which is dependent on the mixture ratio of the polymer and the gas used as the blowing agent. In general extrusion or injection molding processes, the change in viscosity of the polymer determines the process conditions and

the quality of the microcellular foam polymer. However, few studies have focused on the rheological properties obtained when mixing gas and polymers with a blowing agent. Instead, early research into mixing polymers and a blowing agent concentrated on the rheological properties of the gas produced internally from mixing with a chemical blowing agent rather than an inert gas [12]. Since a plunger viscometer was used in this early research to examine a two-phase condition, the pressure profile in the capillary was nonlinear.

The formation of a cell using thermodynamic instabilities in a single-phase gas and resin mixture is the principle behind microcellular foaming. The viscosity change of the polymer and gas mixture is important when designing dies or molds, and it affects the quality of the microcellular foaming products. The viscosity of a single-phase gas and polymer mixture can be measured with a capillary rheometer, but this measurement technique is less accurate than measurements from actual extruders or injection molding machines. Therefore, when researching and developing a microcellular foaming process, one should measure the viscosity against the gas content of the polymer under the various conditions found in an actual process using an extruder or injection-molding machine. Fig. 2 and 3 are experimental results by using extruder capillary test machine.

The influence of a CO_2 blowing agent on resins containing no talc or 20% wt talc is shown in Fig. 2. The resin containing 20% wt talc and 1 or 3% wt gas shows a greater decline in viscosity as the shear rate is increased compared to the resin containing no talc.

Fig. 3 shows the effect of the CO_2 content on resins with 20% talc at various temperatures. The viscosity of the resin with 1% or 3% wt gas at 200°C is less than that of the resin without gas at 210°C. Therefore, using the former can help reduce the process cycle time. In addition, the resin with 3% wt gas at 190°C has a lower viscosity at higher shear rates than that the resin with no gas at 210°C. Therefore, the process temperatures can be set even lower when high shear rates are required.

3.2 Surface tension change in a polymer/Gas mixture

The interfacial properties of binary polymer/CO_2 or polymer/N_2 systems have received considerable attention, especially in the field of polymer foaming in

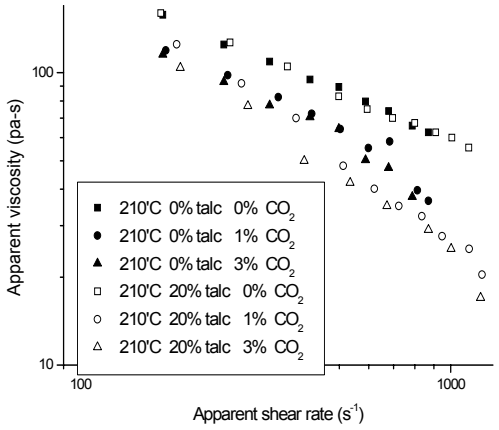

Fig. 2. Influence of the amount of injected gas on the viscosity of each resin at 210°C.

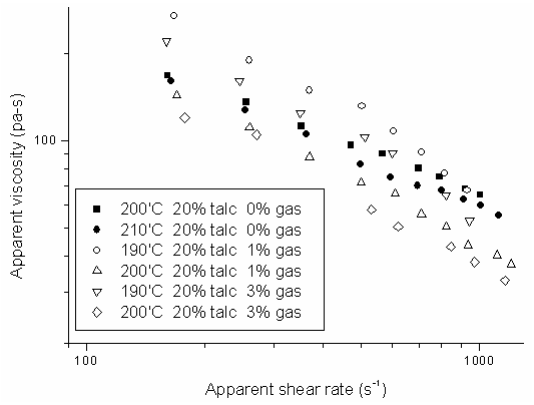

Fig. 3. Effect of CO_2 content on the viscosity change of a resin containing 20% talc at various temperatures.

which CO_2 and/or N_2 are utilized. However, few studies have investigated the surface tension of polymer/scCO_2 systems. Li *et al*. reported the surface tension of polystyrene (PS) and polypropylene (PP) in contact with scCO_2 at 200 to 230°C using the pendant drop method [13]. They also predicted the surface tension of polymers in contact with scCO_2 by applying the surface tension theory developed by Poser and Sanchez [14] with a linear density profile assumption.

However, their predictions showed some discrepancies in CO_2 pressure ranges of 0.1 to 10 MPa. In the present study, the surface tensions of PP, PS, and polylactic acid (PLA) were measured using a simple pendant method with a high-pressure cell, and then compared to the predictions of the Poser and Sanchez [14] surface tension theory using a nonlinear density profile.

The surface tension was calculated by fitting the shape of an experimental drop in an equilibrium state to a theoretical drop profile using Laplace's equation of capillarity,

$$\gamma(\frac{1}{R_1}+\frac{1}{R_2})=\frac{2\gamma}{b}-\Delta\rho gz \quad (22)$$

Where γ is the surface tension, R_1 and R_2 are the principal radii of curvature of the drop, b is the radius of curvature of the drop at the origin, $\Delta\rho$ is the difference in density between the two phases, z is the vertical length from the origin, and g is the gravitational acceleration constant. Fig. 4 indicates the experimental result data for three molten polymers in contact with pressurized CO_2. The surface tension of the molten polymer/CO_2 systems decreased as the CO_2 pressure increased. The predictions were in good agreement at pressures ranging from 5 to 15 MPa. The surface tension theory combined with an equation of state was used to predict the surface tension between the molten polymer and CO_2. The density gradient model developed by Poser and Sanchez [14] was used to correlate surface tension [15].

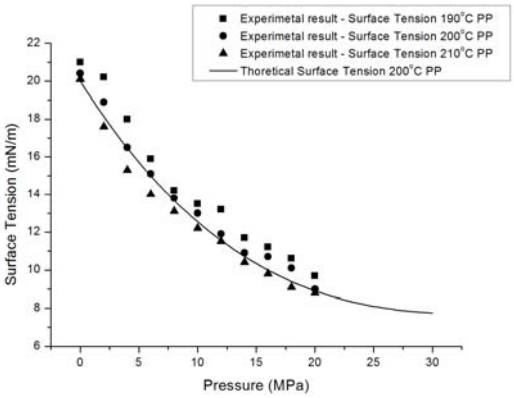

Fig. 4. Surface tension of a polymer/CO_2 mixture.

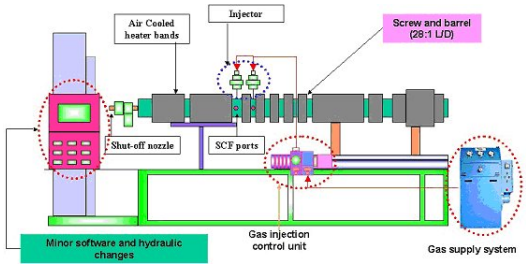

Fig. 5. Schematic diagram of the injection molding machine.

4. Experiments

The injection molding machine (WOOJIN, EX-120) was especially adapted for the microcellular foaming process and equipped with a pressure transducer (Dynisco, PT462E-10M-6/18) to measure the pressure at the barrel as well at the injection port through which gas was injected into the barrel to monitor real-time change in pressure with the gas injection (See Fig. 5). The barrel length to diameter ratio was L/D = 28, which is larger than general injection molding machines so that the gas and polymer would be thoroughly mixed. A high pressure gas supply system was designed to compress N_2 at up to 800 MPa. When the injection molding machine started feeding and the screw started to move, the gas supply system received a signal, set the delay and supply times, and began to supply gas automatically at a fixed flow rate into the injection port. The gas supply pressure was fixed at 340 bar. It was possible to supply a fixed quantity of gas by using a precise mass flowmeter (Bronkhorst, EL-FLOW) by setting the gas supply pressure at 10 to 20 MPa.

The pressure inside the barrel was measured with an indicator (Dynisco, 1290-1-3) connected to the pressure transducer.

A shutoff nozzle was fixed to the end of the barrel to maintain a sufficiently high pressure at which gas was dissolved inside the polymer so that the gas and polymer were not separated into two phases. The shutoff nozzle used a hydraulic pin that was closed until the injection started, based on the interlocking signals received from the injection molding machine.

All of the materials used for this work were commercial products and used as received without any further treatment. The polymer resin in the experiment was PP, which is typically used in car interiors such as the rear door side trim or switch panels. Highly purified N_2 was used as the blowing agent. Fig. 6 shows the standard ASTM sample pieces used to examine the bubble sizes.

5. Results and Discussion

3-D modeling was used to compare the actual size of bubbles observed on the specimens with estimates from the proposed model. Fig. 7 shows the 3-D simulation results under actual injection conditions. The applied gas saturation pressure was 15 or 20 MPa, the injection temperature was 210°C, and the polymer

Fig. 6. ASTM standard sample pieces used for the microcellular injection process.

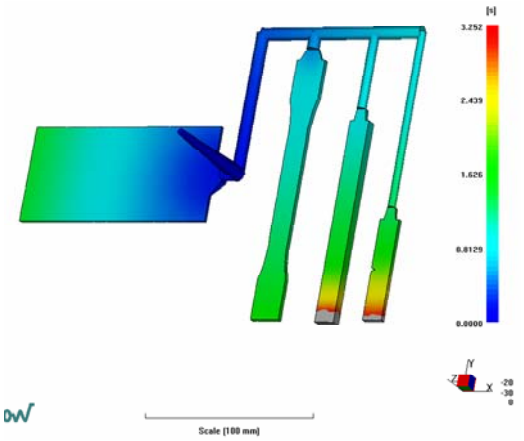

Fig. 7. Simulated bubble growth in a mold using MPI 4.1.

contained 20% talc.

Fig. 8 compares the estimated results from the proposed model with the bubbles observed on the specimen. The bubble growth was altered by the time that polymer remained inside the mold, which depended on the time required for the mold to be filled by the injection nozzle.

Fig. 9 shows scanning electron microscope (SEM) images at different positions in the same specimen. The bubble size varied with the amount of time the polymer spent in the mold. When the polymer was initially injected, the difference between the saturation pressure of the bubbles and the pressure experienced by the polymer near the bubbles was large.

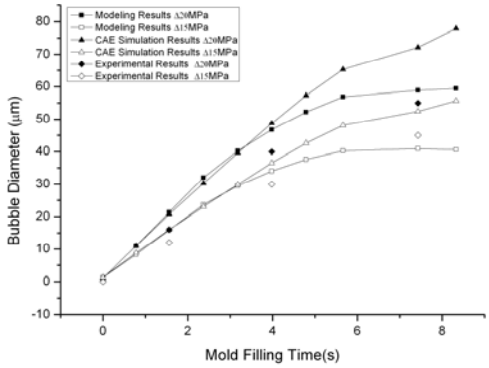

Fig. 8. Comparison of results from CAE simulations and the proposed variable property model.

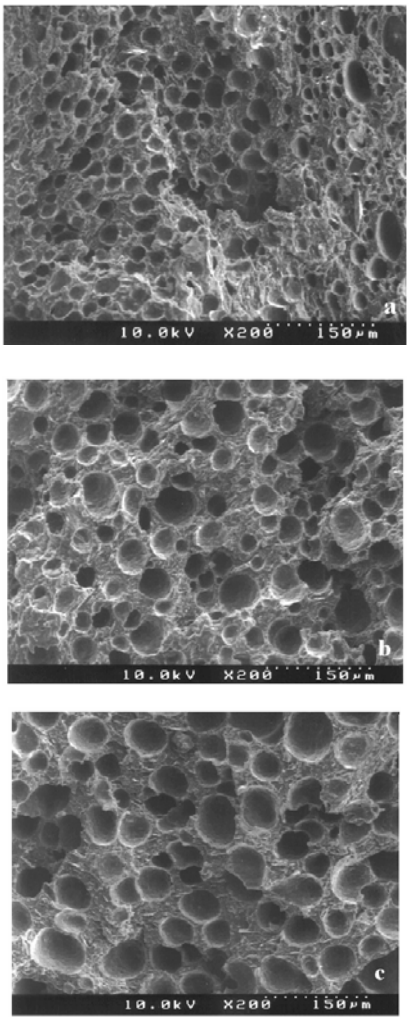

Fig. 9. Bubble size according to the residence time in the injection mold: (a) section closest to the gate, (b) middle section between the gate and the end of the flow, and (c) section at the end of the flow.

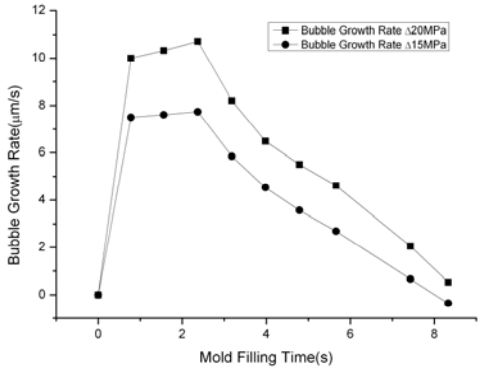

Fig. 10. Relationship between the residence time in the mold and the bubble growth rate at different saturation pressures.

Therefore, the bubble growth was large because the pressure change that contributed to the bubble growth was similar to that under normal atmospheric conditions when the polymer grows freely. However, toward the end of the polymer injection, the bubble growth declined because the saturation pressure difference was small.

Fig. 10 shows the relationship between the residence time in the mold and the bubble growth rate related to the saturation pressure. The higher saturation pressure supplies more energy to create larger bubbles in the mold at the same time. Therefore, the bubble growth rate of 20 MPa saturation pressure process condition is larger than that of 15 MPa saturation pressure process condition.

6. Conclusions

A method for controlling the formation of bubbles in a polymer injection mold is important because the size of the bubbles inside a polymer product has great influence on the resulting contraction and mechanical strength. We therefore require a means of predicting bubble characteristics that considers property changes due to the flow of the polymer in the mold to set the injection process parameters and design the mold.

Most existing analysis methods use a constant viscosity and surface tension to predict the size of the bubbles. Under actual situations, however, when the polymer contains gases, changes occur in the viscosity and surface tension that cause discrepancies between the estimated and observed bubble sizes.

We demonstrated that a model using variable bubble properties predicted bubble sizes that were closer to actual observations compared to results obtained from standard analysis tools. Therefore, the collection and application of basic property change data for polymers during an injection molding process are indispensable when estimating the size of the resulting bubbles to maximize the strength or to decrease the contraction of a product.

References

[1] V. Kumar, Microcellular Polymers: Novel Materials for the 21st Century, *Cellular Polymers*, 12 (3) (1993) 207-223.

[2] D. Ladin, C. B. Park, S. S. Park, H. E. Naguib and S. W. Cha, Study of Shear and Extensional Viscosities of Biodegradable PBS/CO2 Solutions, *J. Cell. Plast.*, 37 (2001) 109-148.

[3] J. E. Martini, F. A. Waldman and N. P. Suh, The Production and Analysis of Microcellular Thermoplastic Foams, *SPE ANTEC Tech papers*, 28 (1982) 674-676.

[4] J. R. Youn and N. P. Suh, Processing of Microcellular Polyester Composites, *Polym. Comp.*, 6 (3) (1985) 175-180.

[5] J. S. Colton and N. P. Suh, Nucleation of Microcellular Foam: Theory and Practice, *SPE ANTEC Tech.*, 32 (1986) 45-47.

[6] J. Mulrooney, *An Investigation of a Sorption Apparatus to Measure the Solubility and Diffusivity of a Liquid Blowing Agent in a Polymer at an Elevated Pressure*, M.A.Sc. Thesis, University of Toronto, (1995).

[7] P. Zoller, Pressure-Volume-Temperature Properties of Three Well-Characterized Low-Density PE, *J. Appl. Polym. Sci.*, 23 (1978) 1051-1056.

[8] M. Amon and C. D. Denson, A Study of the Dynamics of Foam Growth, *Polym. Eng. Sci.*, 24 (13) (1984) 1026-1034.

[9] P. L. Durrill and R. G. Griskey, Diffusion and Solution of Gases in Thermally Softened or Molten Polymers, *AIChE J.*, 12 (6) (1966) 1147-1151.

[10] S. Y. Hobbs, Bubble Growth in Thermoplastic Structural Foams, *Polym. Eng. Sci.*, 16 (4) (1976) 270-275.

[11] L. E. Scriven, On the Dynamics of Phase growth, *Chem. Eng. Sci.*, 10 (1959) 1-13.

[12] C. B. Park, A. H. Behravesh and R. D. Venter, Low Density Microcellular Foam Processing in Extrusion Using CO2, *Polymer Eng. Sci.*, 38 (1998) 1812-1823.

[13] H. Li, L. J. Lee and D. L. Tomasko, Effect of Car-

bon Dioxide on the Interfacial Tension of Polymer Melts, *Ind. Eng. Chem. Res.*, 43 (2004) 509-514.
[14] I. C. Sanchez, Statistical Thermodynamics of Bulk and Surface Properties of Polymer Mixtures, *Macromolecules*, 17 (1980) 565-589.
[15] E. Funami, K. Taki, T. Murakami, S. kihara and M. Ohshima, Measurement and prediction of surface tension of polymer in supercritical CO2, *SPE Conference*, 2 (18) (2006) 245-251.

Yongrak Moon received his B.S., M.S. and Ph.D. degrees from the department of Mechanical Engineering at the Yonsei University in Korea. During his Ph.D., he worked on the Microcellular Foaming Process. Since 2004, he has been employed as a senior researcher at LS Cable Co. Ltd. in Korea. In the company, he worked on the development of an efficient plasticizing unit in injection molding machines and researched advanced polymer processing technology. Currently, he is working on PET foaming and development of open-porous structure polymer product in the Microcellular Plastic Manufacturing Laboratory at the University of Toronto in Canada as a Postdoctoral Fellow.

Sung W. Cha received his Ph.D. degrees from M.I.T. in 1994. He is currently a Professor at the School of Mechanical Engineering at Yonsei University in Seoul, Korea. His research interests include Microcelluar Foaming Process, Axiomatic Design, Manufacturing Process and Idea Development Theory.